JOURNAL OF VIROLOGY, Mar. 1995, p. 1582–1590 Vol. 69, No. 3
0022-538X/95/$04.00+0

Debilitation of Plant Potyvirus Infectivity by P1 Proteinase-Inactivating Mutations and Restoration by Second-Site Modifications

JEANMARIE VERCHOT AND JAMES C. CARRINGTON*

Department of Biology, Texas A&M University, College Station, Texas 77843

Received 14 October 1994/Accepted 23 November 1994

Tobacco etch virus (TEV) encodes three proteinases that catalyze processing of the genome-encoded polyprotein. The P1 proteinase originates from the N terminus of the polyprotein and catalyzes proteolysis between itself and the helper component proteinase (HC-Pro). Mutations resulting in substitution of a single amino acid, small insertions, or deletions were introduced into the P1 coding sequence of the TEV genome. Deletion of the N-terminal, nonproteolytic domain of P1 had only minor effects on virus infection in protoplasts and whole plants. Insertion mutations that did not impair proteolytic activity had no measurable effects regardless of whether the modification affected the N-terminal nonproteolytic or C-terminal proteolytic domain. In contrast, three mutations (termed S256A, F, and Δ304) that debilitated P1 proteolytic activity rendered the virus nonviable, whereas a fourth proteinase-debilitating mutation (termed C) resulted in a slow-infection phenotype. A strategy was devised to determine whether the defect in the P1 mutants was due to an inactive proteinase domain or due simply to a lack of proteolytic maturation between P1 and HC-Pro. Sequences coding for a surrogate cleavage site recognized by the TEV NIa proteinase were inserted into the genome of each processing-debilitated mutant at positions that resulted in NIa-mediated proteolysis between P1 and HC-Pro. The infectivity of each mutant was restored by these second-site modifications. These data indicate that P1 proteinase activity is not essential for viral infectivity but that separation of P1 and HC-Pro is required. The data also provide evidence that the proteinase domain is involved in additional, nonproteolytic functions.

Tobacco etch virus (TEV), a member of the *Potyviridae* family of positive-strand RNA viruses, possesses a genome encoding a single large polyprotein that is proteolytically processed by three virus-specific proteinases (32). The requirement for three proteinases is intriguing, given that there is no conceptual limitation to a polyprotein-producing virus's requiring only a single proteolytic enzyme, as do the como- and nepoviruses (21). At least two selective advantages can be envisioned that might have contributed to the acquisition and maintenance of multiple proteinases through modular evolution (12). First, increasing the number of proteinases may have provided an additional means to regulate proteolysis through differential activities of the enzymes. Second, the different proteinases may have been adopted to provide additional, nonproteolytic viral functions. Several examples are now available to support the latter idea. The picornavirus 3C proteinase exhibits RNA-binding activity that may be necessary for initiation of positive-strand RNA synthesis (2). Additionally, the core domain of the Sindbis virus capsid protein is a serine-type proteinase (11), illustrating that a proteinase can provide both enzymatic and structural functions.

Multiple activities have been assigned to the potyviral proteinases. The NIa proteinase is a picornavirus 3C-like proteinase that recognizes cleavage sites within the C-terminal two-thirds of the polyprotein (6). The proteolytic domain of NIa lies within the C-terminal half of the protein (6, 20), whereas the N-terminal region contains the VPg (viral protein, genome-linked) activity (26, 34). The helper component proteinase (HC-Pro) contains a papain-like proteinase domain near the C terminus (5, 28) and an N-terminal domain required for aphid transmissibility of the virus (3, 35). This proteinase is required for cleavage only at its C terminus.

The potyviral P1 proteinase was characterized recently as a serine-type enzyme that catalyzes cleavage at a Tyr-Ser dipeptide between itself and HC-Pro (25, 38). The C-terminal half (147 amino acid residues) of P1 contains the complete functional proteinase, with a catalytic triad composed of His-214, Asp-223, and Ser-256, whereas the N-terminal 157 amino acid residues are dispensable for proteinase activity (37). The P1 proteinase cleaves preferentially by an autoproteolytic mechanism, and its activity in vitro requires a cellular factor present in extracts from plant (wheat germ) but not animal (rabbit reticulocyte) cells (37). The P1 protein was shown to exhibit nonspecific RNA-binding activity (4), although the domain required for this function is not known. Among different potyviruses, the P1 protein is the least conserved region of the entire polyprotein (16, 36). In fact, the N-terminal half of P1 is hypervariable both in length and in sequence.

To understand the role of the potyvirus P1 protein in viral infectivity, TEV mutants containing altered P1 coding sequences were generated. Mutants containing substitutions, insertions, or deletions in the proteolytic and nonproteolytic domains of P1 were analyzed for their abilities to infect isolated cells and whole plants. The mutant genomes also encoded a reporter protein, β-glucuronidase (GUS), which allowed quantitative analysis of viral replication and movement through plants.

MATERIALS AND METHODS

Strains, plants, and plasmids. Most recombinant and mutagenized plasmids were cloned in *Escherichia coli* HB101. Single-stranded plasmid DNA was prepared from *E. coli* RZ1032 by infection with the defective phage M13K07. Complementary DNA representing the TEV genome was described previously (15). The numbering of all TEV nucleotides and amino acid residues, starting from the genome 5′ end and N terminus of the polyprotein, respectively, was based on the published sequence (1). *Nicotiana tabacum* cv. Xanthi nc was used for all whole-plant infections and protoplast isolations.

A series of eight mutations, resulting in three-amino-acid insertions in the P1 protein, were generated by oligonucleotide-directed mutagenesis (23) with the

* Corresponding author. Phone: (409) 845-2325. Fax: (409) 845-2891. Electronic mail address: carrington@bio.tamu.edu.

intermediate plasmid pTL7SN.3-0027DA-GUS (15). This plasmid contains an SP6 promoter adjacent to cDNA representing TEV nucleotides 1 to 2681, with the GUS coding sequence inserted between the P1 and HC-Pro regions. This plasmid also contains cDNA from the 3′-terminal 152 nucleotides of the genome plus a poly(A)$_{45}$ sequence immediately downstream from the larger TEV sequence. The insertions consisted of nine nucleotides (ACCATGGCA), containing an *Nco*I site and encoding a Thr-Met-Ala tripeptide. The sites of insertion were after nucleotides 429, 522, 561, 615, 708, 792, 885, and 972 and were chosen by a semirandom process that ensured that insertions were spaced no greater than 100 nucleotides apart. These insertions were designated with the letter codes A1, A2, A, B, C, D, E, and F, respectively. The S256A mutation, resulting in substitution of Ala for Ser-256 at the active site of the P1 proteinase, was described previously (38) and was subcloned into pTL7SN.3-0027DA-GUS by using a *Bsi*WI-*Bsi*WI restriction fragment containing TEV nucleotides 479 to 940.

Three deletion mutations were produced by using pTL7SN.3-0027DA-GUS. The Δ05 and Δ06 deletions were generated by removal of sequence between the *Nco*I site flanking the start codon of the TEV open reading frame and the introduced *Nco*I sites after nucleotides 561 and 615, respectively. The Δ304 deletion, which eliminated Tyr-304 at the C-terminal position of P1, was also described previously (37).

Oligonucleotide-directed mutagenesis was conducted with pTL7SN.3-0027DA-GUS plasmids carrying the S256A and F mutations to introduce the sequence ACTGAGAATCTTTATTTTCAGAGC between the coding regions for P1 and GUS. This insertion codes for Thr-Glu-Asn-Leu-Tyr-Phe-Gln-Ser, the last seven amino acid residues of which function as an NIa proteinase recognition site, with proteolysis occurring between the Gln and Ser residues (7, 17, 19). The names of all plasmids containing the NIa cleavage site coding sequence at this position were given the suffix P1 ↓ G.

The plasmid pTL7SN.3-0027DA-G ↓ H contains the coding sequence for the NIa cleavage site between the GUS and HC-Pro regions and was described previously (10). The C, F, S256A, and Δ304 mutations were introduced into pTL7SN.3-0027DA-G ↓ H by site-directed mutagenesis.

Each point, insertion, and deletion mutation was introduced into a plasmid containing the full-length TEV cDNA by the following strategy. The intermediate plasmid pTL7SN.3-0027DA-GUS, containing the P1 mutations, and similar plasmids containing the NIa cleavage recognition sequences were digested with *Bst*EII, which cleaves the adjacent 5′ and 3′ cDNA fragments at TEV nucleotide positions 1430 and 9467, respectively. The *Bst*EII-*Bst*EII fragment corresponding to nucleotides 1430 to 9467 was excised from the full-length cDNA of pTEV7DA (15) and inserted into the *Bst*EII-digested pTL7SN.3-0027DA-GUS derivative. All plasmids containing a full-length TEV cDNA and the GUS sequence were named with the prefix pTEV7DAN-GUS. The plasmid pTEV7DAN-GUS/VNN, containing a mutation resulting in substitution of Val-Asn-Asn for the highly conserved Gly-347–Asp-348–Asp-349 in NIb polymerase, was described previously (10).

Four plasmids were constructed to analyze the GUS activity of P1/GUS, GUS/HC-Pro, and P1/GUS/HC-Pro fusion proteins in protoplasts. pRTL2, the base vector for these plasmids, contains a cauliflower mosaic virus 35S transcriptional promoter and terminator (9). pRTL2-0027GUS contains an insertion of cDNA representing TEV nucleotides 1 to 2681, including the GUS coding sequence introduced between the P1 and HC-Pro coding regions. pRTL2-0027GUS/S256A is identical to pRTL2-0027GUS except for a mutation converting the Ser-256 codon in P1 to one coding for Ala. pRTL2-P1GUS contains the coding regions for P1 and GUS, including a functional P1 cleavage site. pRTL2-P1GUS/303 is similar to pRTL2-P1GUS except that the P1-GUS fusion junction lacks the sequence coding for Tyr-304 in P1, rendering the cleavage site between P1 and GUS inactive (37). These plasmids were used for transient-expression analysis in protoplasts as described previously (8).

In vitro transcription and translation. All transcripts were synthesized by using SP6 RNA polymerase and plasmids purified by CsCl gradient centrifugation. Transcripts used to program in vitro translation reactions were synthesized from *Bst*EII-linearized plasmids. In vitro translation was carried out for 1 h at 25°C with commercially prepared wheat germ extract (Promega) in the presence of [^{35}S]methionine (NEN-DuPont). After some translation reactions, NIa proteinase was added and incubation was continued for 1 h at 30°C. The proteinase contained six His residues at the N terminus and was purified from a recombinant *E. coli* strain by Ni^{2+} affinity chromatography as described before (29). Full-length transcripts were synthesized in the presence of 7-methylguanosine-5′-triphospho-5′-guanosine by using *Bgl*II-linearized DNA (15). Transcripts were used directly for whole-plant inoculations or concentrated fivefold by precipitation with 2 M LiCl for protoplast inoculations (13).

Plant and protoplast inoculations. The relative amounts of parental and mutant transcripts used in each experiment were normalized. Tobacco plants were inoculated with transcripts (10 to 20 μg) by mechanical abrasion as in earlier studies (13, 15). Tobacco protoplasts were prepared and inoculated by the polyethylene glycol procedure as described before (8, 27) and maintained at room temperature under constant fluorescent light.

Analysis of virus infection. Protoplasts were harvested at 24, 48, and 72 h postinoculation (h.p.i.) by centrifugation and resuspended in GUS lysis buffer (40 mM sodium phosphate, 10 mM EDTA, 0.1% Triton X-100, 0.1% sodium lauryl sarcosine, 0.07% β-mercaptoethanol [pH 7.0]). GUS activity was assayed by using the fluorometric substrate 4-methylumbelliferyl-β-D-glucuronide as described before (8, 22). Activity values (picomoles of substrate cleaved per minute per 10^5 protoplasts) were calculated from averages of replicate, contemporaneous samples, and the data were analyzed with a two-sample *t* test with the StatView 4.0 program (Abacus Concepts, Inc.).

Virus infectivity in whole plants was analyzed by GUS activity assays as described above; an immunoblot assay with anticapsid, anti-HC-Pro, and anti-GUS sera (30); and by reverse transcriptase-PCR (RT-PCR) and nucleotide sequencing (14). In some experiments, GUS activity in inoculated or systemically infected leaves was analyzed in situ by using the histochemical substrate 5-bromo-4-chloro-3-indolyl-β-D-glucuronic acid cyclohexylammonium salt (X-gluc) and the vacuum infiltration technique (15). For immunoblot assays, 1 g of upper noninoculated leaves was ground in 5 ml of protein dissociation buffer (0.063 M Tris-HCl [pH 6.8], 2% sodium dodecyl sulfate [SDS], 10% 2-mercaptoethanol, 10% glycerol). Extracts were subjected to SDS–12.5% polyacrylamide gel electrophoresis, after which the proteins were transferred to nitrocellulose membranes and incubated with antisera. Positive reactions were detected by using a chemiluminescence system (Amersham, Inc.).

To conduct RT-PCR analysis, virus extracts were prepared from upper, noninoculated leaves obtained at 14 days postinoculation (d.p.i.) as described before (18) but with the exclusion of the CsCl gradient step. Viral RNA was isolated by proteinase K treatment followed by phenol extraction and ethanol precipitation. With RNA from Δ05 and Δ06 mutant-inoculated plants, RT-PCRs were carried out with a first-strand primer complementary to GUS nucleotides 387 to 407 and a second-strand primer corresponding to TEV nucleotides 123 to 142 in the 5′ noncoding region. Two separate RT-PCRs were conducted with RNA from C, F, S256A, or Δ304 mutant-inoculated plants. The first reaction used the same first-strand primer described above but a second-strand primer corresponding to TEV nucleotides 523 to 538. The second RT-PCR used a first-strand primer complementary to TEV nucleotides 2396 to 2415 within the HC-Pro coding region and a second-strand primer corresponding to GUS nucleotides 1761 to 1778. Nucleotide sequencing of RT-PCR products was conducted to verify the presence or absence of the P1 mutations, the NIa cleavage site insertion between P1 and GUS sequences, and the NIa cleavage site insertion between GUS and HC-Pro sequences.

RESULTS

Mutations in the P1 protein-coding region of the TEV genome. Twelve mutations were introduced into the P1 coding region of pTEV7DAN-GUS, the full-length TEV cDNA-containing plasmid from which parental TEV-GUS derives (15). Eight insertions, each consisting of nine nucleotides encoding the tripeptide Thr-Met-Ala, were introduced separately into the P1 region at approximately 90-bp intervals and were represented by the letter codes indicated in Fig. 1A. Insertions A1, A2, and A modified the N-terminal nonproteolytic region, while the remaining insertions affected the proteolytic domain. Notably, mutation F resulted in an insertion between Phe-276 and Ile-277 within the sequence Phe-Ile-Val-Arg-Gly, a motif that is highly conserved among potyviruses, deletion of which was shown to inhibit P1 proteolysis (38). A substitution mutation (S256A) resulted in conversion of Ser-256 to Ala at the P1 active site and was shown previously to inactivate the proteinase (38). Three deletion mutations, resulting in removal of 139 or 157 amino acid residues from the nonproteolytic domain (Δ05 and Δ06, respectively) or only the C-terminal Tyr-304 residue, were also introduced (Fig. 2A).

To analyze the effects of these mutations on P1 processing, transcripts from *Bst*EII-linearized plasmids were translated in a wheat germ extract. Transcripts from the parental plasmid and those containing the insertion and substitution mutations encoded a 117-kDa polyprotein consisting of P1, GUS, and a 14-kDa segment of HC-Pro. Translation of transcripts encoding an active P1 proteinase should result in the accumulation of the 35-kDa P1 protein and the 82-kDa GUS/HC-Pro fusion protein. Processed products were detected after translation of transcripts from the parental plasmid as well as A1, A2, A, B, D, and E mutant plasmids (Fig. 1B). Translation of transcripts from S256A, C, and F mutant plasmids resulted in accumulation of a stable 117-kDa polyprotein (Fig. 1B), even after an additional 15 h of incubation. The inhibitory effects of the

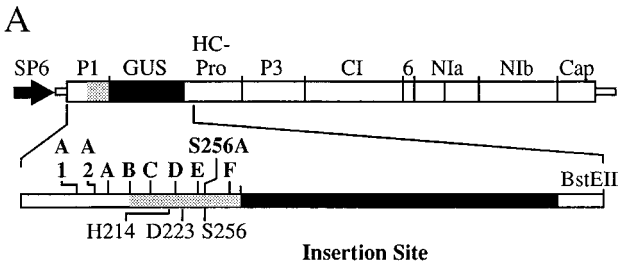

Insertion Site	nt.	a.a.
A1	429	95
A2	522	126
A	561	139
B	615	157
C	708	188
D	792	216
E	885	247
F	972	276

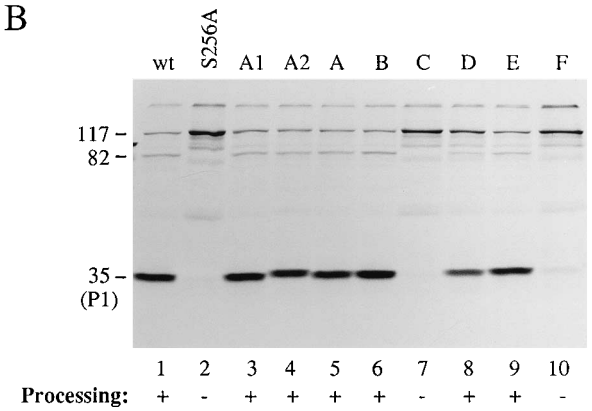

FIG. 1. Mutations in the TEV P1 coding region and their effects on P1 proteolytic activity. (A) Diagrammatic representation of relevant portions of the pTEV7DAN-GUS plasmid, including the SP6 promoter, TEV genomic cDNA (open box), and the GUS coding sequence (solid box). The coding region for the proteolytic domain of P1 is indicated by the stippled box. The positions of sequences encoding P1, HC-Pro, and NIa proteinase cleavage sites are indicated by vertical lines. The N-terminal coding sequence (to the *Bst*EII site) is enlarged, and the relative positions of P1 mutations are indicated by the letters. The positions of codons for the proposed active-site residues (His-214, Asp-223, and Ser-256) in the P1 proteinase are shown below the enlargement. The nucleotide (nt) and corresponding amino acid (a.a.) insertion site positions within the P1 sequence are listed below the diagram. Abbreviations: P1, protein 1; HC-Pro, helper component proteinase; P3, protein 3; CI, cylindrical inclusion protein; 6, 6-kDa protein; NIa, nuclear inclusion protein a; NIb, nuclear inclusion protein b; Cap, capsid protein. (B) Cell-free translation and processing products encoded by transcripts from *Bst*EII-linearized plasmids containing the P1 mutations. Translation reaction mixes were programmed with parental (wt) or mutant transcripts, as indicated above each lane. [^{35}S]methionine-labeled translation products were analyzed by SDS–12.5% polyacrylamide gel electrophoresis and fluorography. The electrophoretic positions of the 117-kDa P1/GUS/partial HC-Pro polyprotein, the 82-kDa GUS/partial HC-Pro fusion protein, and the 35-kDa P1 protein are indicated on the left. Whether or not processing occurred to generate the P1 protein is indicated below each lane.

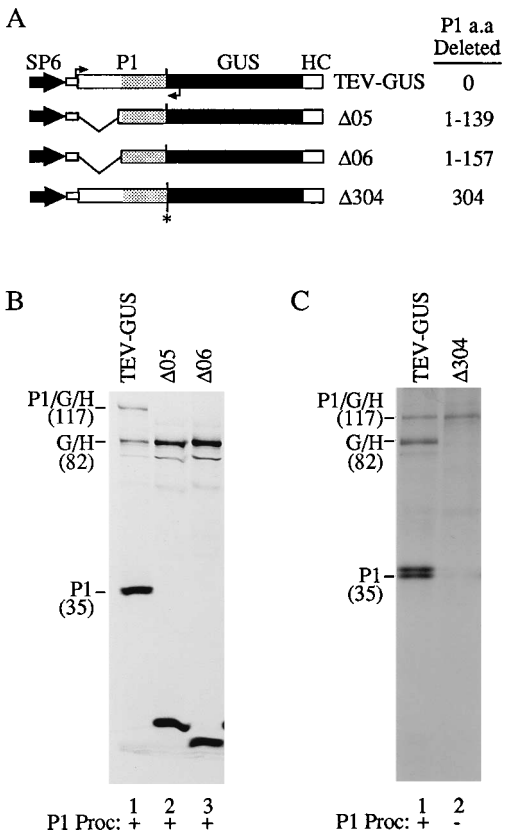

FIG. 2. Deletion mutations in the TEV P1 coding region and their effects on P1 proteolytic activity. (A) Diagrammatic representation of relevant portions of parental and deletion mutant plasmids, including the SP6 promoter, TEV genomic cDNA (open box), and the GUS coding sequence (solid box). The coding region for the proteolytic domain of P1 is indicated by the stippled box. Note that the Δ304 mutant lacks the coding sequence for only Tyr-304. The positions corresponding to RT-PCR primer sites (bent arrows) are indicated in the TEV-GUS diagram. Abbreviations are the same as in the Fig. 1 legend. (B and C) Cell-free translation and processing products encoded by transcripts from *Bst*EII-linearized plasmids containing deletions within the P1 sequence. Translation reaction mixes were programmed with parental (TEV-GUS) or mutant transcripts, as indicated above each lane. [^{35}S]methionine-labeled translation products were analyzed by SDS–12.5% polyacrylamide gel electrophoresis and fluorography. The electrophoretic positions of the 117-kDa P1/GUS/partial HC-Pro polyprotein (P1/G/H), the 82-kDa GUS/partial HC-Pro fusion protein (G/H), and the 35-kDa P1 protein are indicated on the left of each panel. The truncated P1 proteins processed from the Δ05 and Δ06 polyproteins are shown near the bottom of panel B. The P1 processing phenotype of each mutant is indicated below the lanes.

S256A and F mutations were consistent with previously published results (38).

Translation of transcripts from the Δ05 and Δ06 deletion mutant plasmids resulted in processed products corresponding to truncated but proteolytically active P1 polypeptides and the GUS/HC-Pro fusion product (Fig. 2B). Conversely, translation of transcripts from the Δ304 mutant plasmid resulted in accumulation of only the 117-kDa P1/GUS/HC-Pro polyprotein (Fig. 2C).

GUS as a reporter. In previous studies, the GUS reporter was used extensively as a quantitative tool to measure parental and mutant TEV genome amplification in inoculated protoplasts (10, 13, 31). As GUS and TEV proteins are synthesized in stoichiometric quantities, and since TEV proteins and genomic RNA accumulate proportionally (14), GUS is a particularly useful reporter of genome amplification. Parental TEV-GUS encodes a polyprotein in which proteolysis by P1 and HC-Pro results in accumulation of a stable GUS/HC-Pro fusion product (15). The P1 proteinase-defective mutants, however, encode a polyprotein in which P1 fails to autoproteolytically separate from GUS, yielding a stable P1/GUS/HC-Pro polyprotein.

To compare the relative activities of proteins containing P1 and/or HC-Pro fused to GUS, four plasmids suitable for transient-expression analysis in protoplasts were constructed. Two plasmids encoded P1-active polyproteins that resulted in production of nonfused GUS (pRTL2-P1GUS) or GUS/HC-Pro

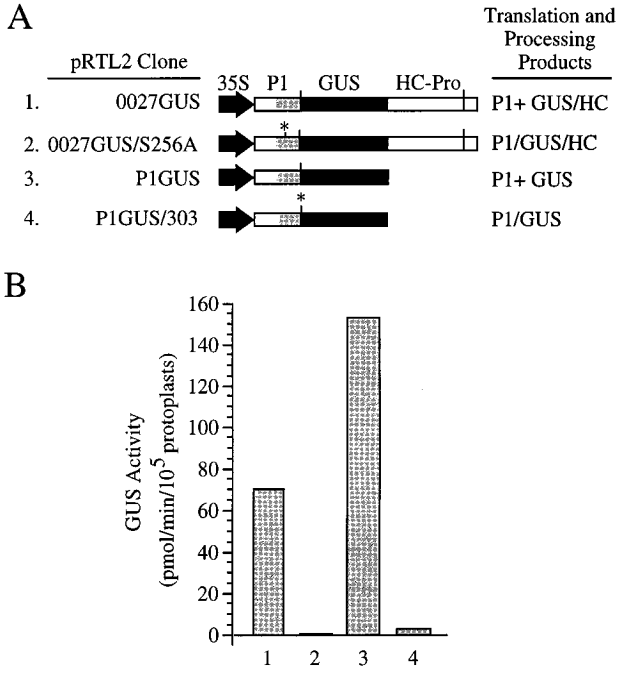

FIG. 3. Relative GUS activity of four polyproteins containing P1, GUS, and HC-Pro. (A) Diagrammatic representation of relevant portions of four pRTL2-based plasmids, including the cauliflower mosaic virus 35S promoter and the coding sequences for P1, GUS, and HC-Pro. The positions of the P1 proteinase-debilitating S256A and 303 mutations are indicated by the asterisks. The identity of each pRTL2-derived plasmid is indicated on the left. The translation and processing products derived from these plasmids are indicated on the right. (B) GUS activity in tobacco protoplasts transfected with each pRTL2-derived plasmid. The numbers below each column correspond to the construct number in panel A. Cells were harvested and GUS activity was measured at 24 h posttransfection. The data shown are averages for three contemporaneous transfections.

(pRTL2-0027GUS) (Fig. 3A). Two additional plasmids encoded P1-inactive polyproteins corresponding to P1/GUS/HC-Pro (pRTL2-0027GUS/S256A) and P1/GUS (pRTL2-P1GUS/303) (Fig. 3A). Protoplasts were transfected with equivalent amounts of plasmid DNA, and GUS activity was measured after 24 h. Whereas the activity in protoplasts accumulating nonfused GUS or GUS/HC-Pro fusion protein was relatively high and differed by only a factor of 2 (Fig. 3B, columns 1 and 3), the activity in protoplasts accumulating P1/GUS or P1/GUS/HC-Pro fusion proteins was markedly low (Fig. 3B, columns 2 and 4). In fact, GUS activity directed by P1/GUS/HC-Pro (column 2) was nearly 350 times lower than that directed by GUS/HC-Pro (column 1). These data strongly suggest that fusion of P1 to the N terminus of GUS inhibits GUS activity in vivo, although fusion of HC-Pro to the C terminus has relatively little effect. Consequently, the GUS activity assay to measure genome amplification in protoplasts was used only for the proteolytically active P1 mutants.

Infectivity of proteolytically active P1 mutants. Amplification of the six insertion mutant (A1, A2, A, B, D, and E) and two deletion mutant (Δ05 and Δ06) genomes encoding active P1 proteinases was measured by using the fluorometric GUS assay. Protoplasts were inoculated with transcripts synthesized from *Bgl*II-linearized plasmids, and GUS activity was quantified at 24, 48, and 72 h.p.i. In each experiment, transcripts representing TEV-GUS were used as the positive amplification control, while transcripts representing TEV-GUS/VNN were used as negative amplification controls. The latter contained a mutation inactivating the viral RNA polymerase (NIb); transcripts from these plasmids were shown previously to be amplification defective (10).

Parental TEV-GUS and each of the six insertion mutant genomes were amplified in protoplasts, with similar accumulation profiles over the 72-h incubation (Fig. 4A to D). None of these mutants was significantly different from TEV-GUS ($P > 0.25$). The Δ05 and Δ06 deletion mutant genomes were also amplified, although at levels lower than that of TEV-GUS (Fig. 4E). The modest reduction in amplification levels was consistent in multiple experiments, although the differences between these deletion mutants and parental virus were not always statistically significant ($0.037 < P < 0.49$). It is important to note that valid comparisons of parental and mutant genome amplification were made with data from concomitant infections with the same protoplast preparation. Protoplasts prepared from different plants varied in their apparent susceptibility, as reflected in the differences in absolute GUS activity levels in the different panels of Fig. 4; however, relative levels of parental and mutant genome amplification were consistent in different experiments.

Tobacco plants were inoculated mechanically with transcripts representing parental TEV-GUS and each of the P1 proteolytically active insertion and deletion mutants. Plants were assayed for infection by visual observation of symptoms and analysis of GUS activity in upper, noninoculated leaves at 14 d.p.i. Parental TEV-GUS and each of the insertion mutants infected at least 70% of the plants inoculated, with systemic symptoms appearing at 5 to 7 d.p.i. (Table 1). Both the Δ05 and Δ06 mutants were infectious, even though they lacked approximately half of the P1 sequence. The infectivity of these two deletion mutants was further verified by RT-PCR analysis with extracts from systemically infected leaves. The 5′ primer corresponded to sequences within the 5′ nontranslated region, while the 3′ primer was complementary to sequences within the GUS coding region. Products of approximately 1,317, 899, and 845 bp were amplified from extracts of plants infected by TEV-GUS, the Δ05 mutant, and the Δ06 mutant, respectively, confirming the viability of the Δ05 (lacking 418 nucleotides) and Δ06 (lacking 472 nucleotides) mutants (data not shown). These data indicate that the N-terminal nonproteolytic domain is dispensable for genome amplification and systemic infectivity.

Infectivity of the proteolytically defective P1 mutants. Because of the low activity of P1/GUS fusion proteins (Fig. 3), GUS was not a useful reporter of genome amplification for the P1 proteinase-defective mutants. Additionally, immunoblot and RNA blot analyses were insufficiently sensitive to quantify viral protein and RNA accurately after inoculation of protoplasts with synthetic transcripts (data not shown). Therefore, the proteolytically inactive mutants were analyzed only in whole plants. Tobacco plants were inoculated with transcripts corresponding to the S256A, C, F, and Δ304 mutants, and immunoblot analysis with anticapsid serum was conducted to analyze infection in upper, noninoculated leaves at 14 and 32 d.p.i. Virus was not detected at either time point in plants inoculated with the S256A, F, or Δ304 mutant (Table 2). No virus was detected at 14 d.p.i. in systemic tissue of plants inoculated with the C mutant, but 17% of C mutant-inoculated plants became systemically infected by 32 d.p.i. (Table 2). This mutant induced mild symptoms, and the amount of capsid protein was relatively low compared with that of the parental virus. A low level of GUS activity was also detected in systemically infected leaves at 32 d.p.i.

Infection by the C mutant was analyzed further by in situ histochemical GUS assays (15) to visualize infection sites in inoculated and systemic leaves at 4, 8, 16, and 32 d.p.i. (Fig. 5).

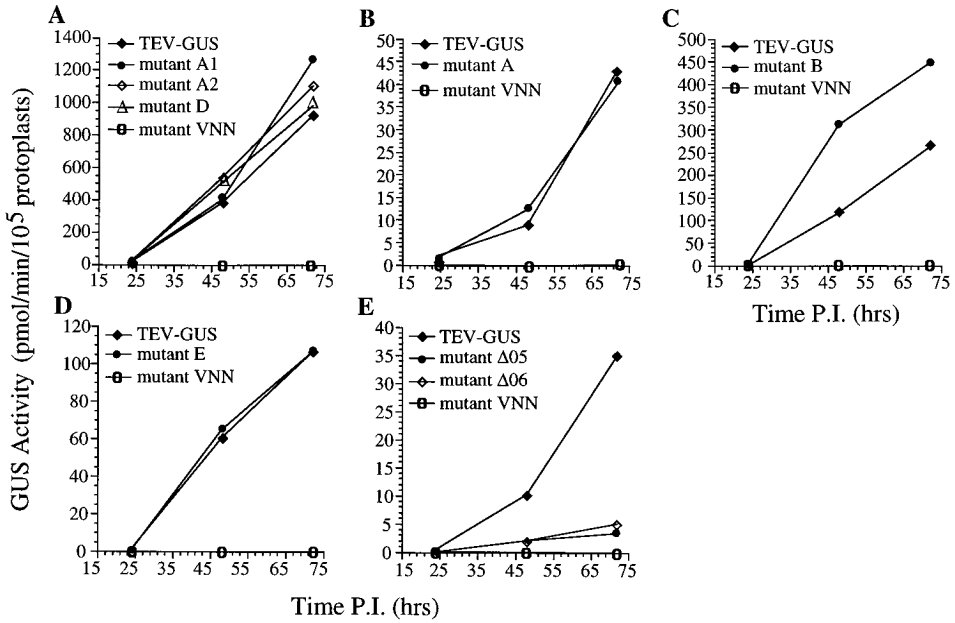

FIG. 4. Amplification of parental and P1 mutant genomes in protoplasts. GUS activity was measured at 24, 48, and 72 h.p.i. The data shown in each panel are averages from one of two or three replicated experiments. All mutants were tested in parallel with parental TEV-GUS and VNN mutant genomes as positive and negative amplification controls, respectively.

At 4 d.p.i., parental TEV-GUS had spread from the initial infection foci to secondary sites through the vasculature of the inoculated leaves (Fig. 5A). Infection foci of the C mutant were confined to an average diameter of six epidermal cells (Fig. 5A). At 8 d.p.i., the C mutant foci had enlarged to diameters averaging 31 epidermal cells, with no detectable vasculature-associated movement (Fig. 5B). The C mutant appeared to invade vasculature-associated cells by 16 d.p.i., although sites distal to the initial infection foci remained free of virus (Fig. 5C). Invasion of the C mutant into systemic leaves was detected at 32 d.p.i. (Fig. 5D). Compared with that by the parental virus, the extent of systemic infection by the C mutant was limited. Because of the low level of C mutant virus in these plants, immunoblot analyses with anti-GUS and anti-HC-Pro sera to determine whether P1 proteinase was partially active in vivo were inconclusive.

Introduction of NIa cleavage sites to restore processing. There are several possible reasons for the correlation between inactivation of the P1 proteinase and debilitation of infectivity in plants. First, successful infection may require that the P1 proteinase and HC-Pro be separated or that a mature C terminus of P1 be formed. As TEV-GUS, which encodes a stable GUS/HC-Pro fusion protein in infected cells, is clearly viable, there appears to be no strict requirement for formation of a mature HC-Pro N terminus. Second, infection may depend on the P1 proteinase's cleaving additional polyprotein sites besides the one located at the C terminus of P1. At present, no such sites have been identified. Third, additional, nonproteolytic functions of the proteolytic domain may be debilitated by mutations that also inactivate the P1 proteinase.

To determine if there is a requirement for an active P1 proteinase or merely for separation of P1 from HC-Pro, sequences coding for NIa-mediated cleavage sites were introduced into the proteinase-debilitated mutant genomes as well as into the parental TEV-GUS genome. The NIa sites were inserted at either of two positions in the viral genomes. The first position was between the GUS and HC-Pro sequences, resulting in TEV-G↓H (wild-type P1), TEV-G↓H/S256A, TEV-G↓H/C, TEV-G↓H/F, and TEV-G↓H/Δ304 (Fig. 6A). As shown previously, a functional cleavage site at this position facilitates separation of HC-Pro from P1 and GUS by NIa-mediated proteolysis (10). The second cleavage site insertion position was between P1 and GUS, resulting in the TEV-P1↓G derivatives (Fig. 6A). A cleavage site at this position

TABLE 1. Infectivity of proteolytically active P1 mutants in plants

Inoculum	No. of plants infected/ no. inoculated[a]	Onset of symptoms (d.p.i.)
TEV-GUS	72/79	5–6
A1	7/10	7
A2	10/10	5
A	10/10	6
B	19/20	6
D	7/10	7
E	8/10	6
Δ05	5/13	7
Δ06	11/16	7

[a] The appearance of symptoms and detection of GUS activity in upper, noninoculated leaves were scored as a positive infection.

TABLE 2. Infectivity of proteolytically defective P1 mutants in plants

Inoculum	No. of plants infected/ no. inoculated[a]	Onset of symptoms (d.p.i.)
TEV-GUS	7/7	6
S256A	0/10	
F	0/10	
C	2/12	32
Δ304	0/10	

[a] The appearance of symptoms and detection of coat protein by immunoblot analysis of extracts from upper, noninoculated leaves at 32 d.p.i. were scored as a positive infection.

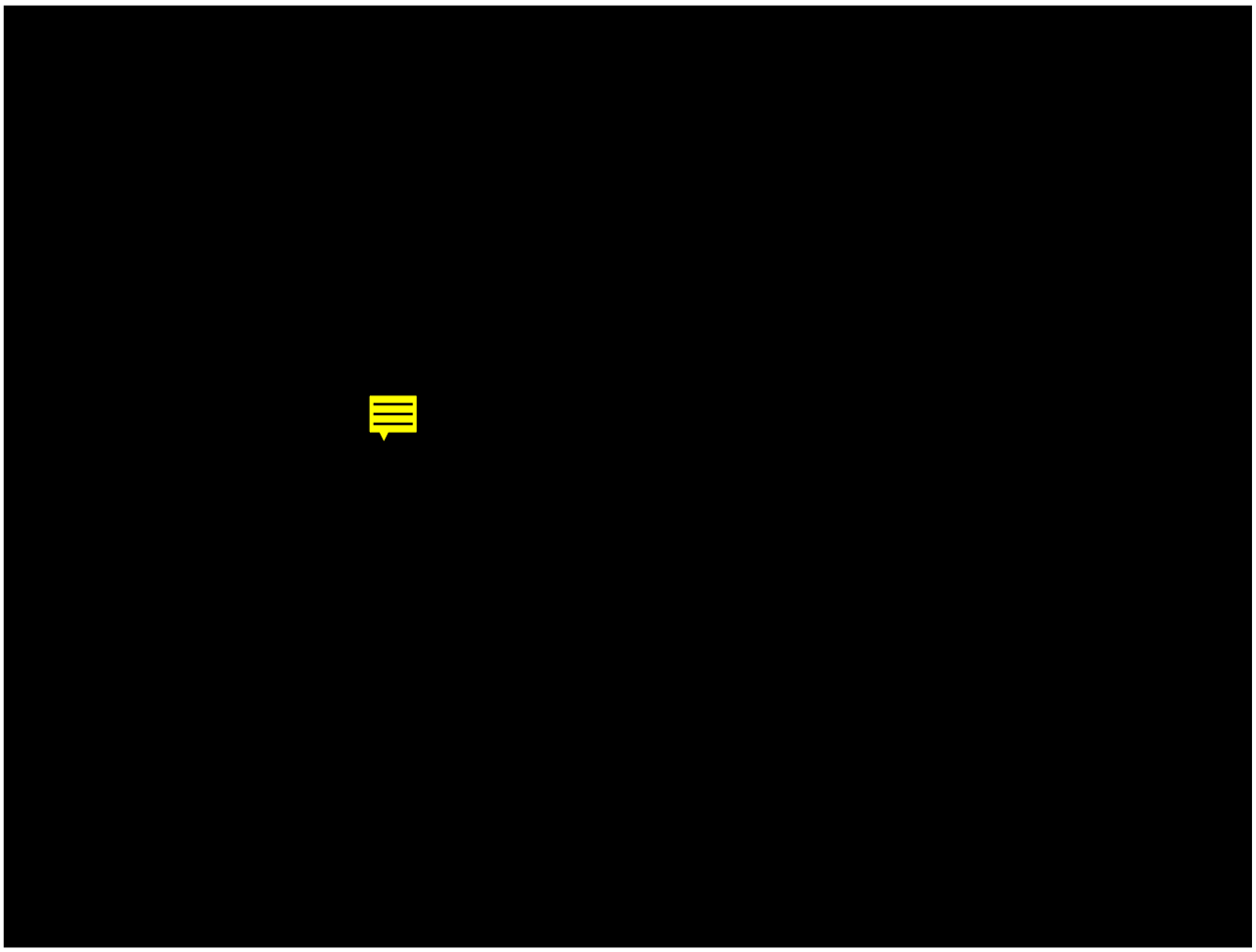

FIG. 5. In situ localization of GUS activity in leaves of plants inoculated with parental TEV-GUS or mutant C transcripts. Inoculated or systemically infected leaves were vacuum infiltrated with X-gluc substrate at 4, 8, 16, and 32 d.p.i. The blue areas indicate sites of infection. The infecting virus (TEV-GUS or mutant C virus) is indicated below each panel.

should result in separation of mature P1 from GUS/HC-Pro. Therefore, these viruses permit investigation of the requirement for proteolytic separation of P1 and HC-Pro independently of the requirement for P1 proteolytic activity.

To verify that the introduced cleavage sites were functional, translation products were synthesized from transcripts of *Bst*EII-linearized plasmids corresponding to each of the parental or modified genomes and reacted with purified NIa proteinase. The transcripts encoded a P1/GUS/partial HC-Pro polyprotein (117 kDa). Figure 6B shows the results of translation and processing of the parental and S256A derivatives. In the absence of NIa proteinase, each of the P1 proteolytically active derivatives yielded mature P1 and GUS/HC-Pro (Fig. 6B, lanes 2, 4, and 6), whereas the 117-kDa polyproteins encoded by the S256A derivatives were stable (lanes 3, 5, and 7). As noted in previous studies (37, 38), the P1 protein migrated during electrophoresis as a doublet. Translation products derived from transcripts of TEV-GUS and its S256A counterpart were unaffected by NIa proteinase (Fig. 6B, compare lanes 2 and 3 with 9 and 10). In contrast, translation products from transcripts of TEV-G ↓ H and its S256A derivative were processed by NIa, yielding mature GUS and P1/GUS fusion protein, respectively (lanes 11 and 12). Translation products from transcripts of TEV-P1 ↓ G and its S256A counterpart were also processed by NIa. In the TEV-P1 ↓ G/S256A polyprotein, P1 and GUS/HC-Pro were generated (Fig. 6B, lane 14), with the electrophoretic mobility of P1 decreased slightly by the additional sequence from the NIa cleavage site. The parental TEV-P1 ↓ G polyprotein contained a functional P1 proteinase cleavage site plus the NIa cleavage site, and in a minor percentage of these polyproteins the NIa site was the only one processed (lane 13). The functionality in vitro of the introduced NIa cleavage sites encoded by the C, F, and Δ304 mutant genomes was also confirmed (data not shown).

To test the abilities of the modified viruses to infect tobacco systemically, upper leaves of transcript-inoculated plants were analyzed at 14 d.p.i. by either immunoblot assay with anticapsid serum or RT-PCR to detect viral RNA corresponding to a 947-nucleotide region containing both P1 and GUS sequences. At least 86% of plants inoculated with transcripts representing the parental viruses encoding an active P1 proteinase, either with (TEV-G ↓ H and TEV-P1 ↓ G) or without (TEV-GUS) an introduced NIa cleavage site, were infected (Table 3). As noted above, the proteolytically inactive TEV-GUS/S256A mutant was unable to infect plants systemically. However, the S256A mutants containing the NIa cleavage site insertions were viable, infecting at least 73% of inoculated plants (Table 3). While the TEV-GUS/Δ304 mutant was inactive, the TEV-

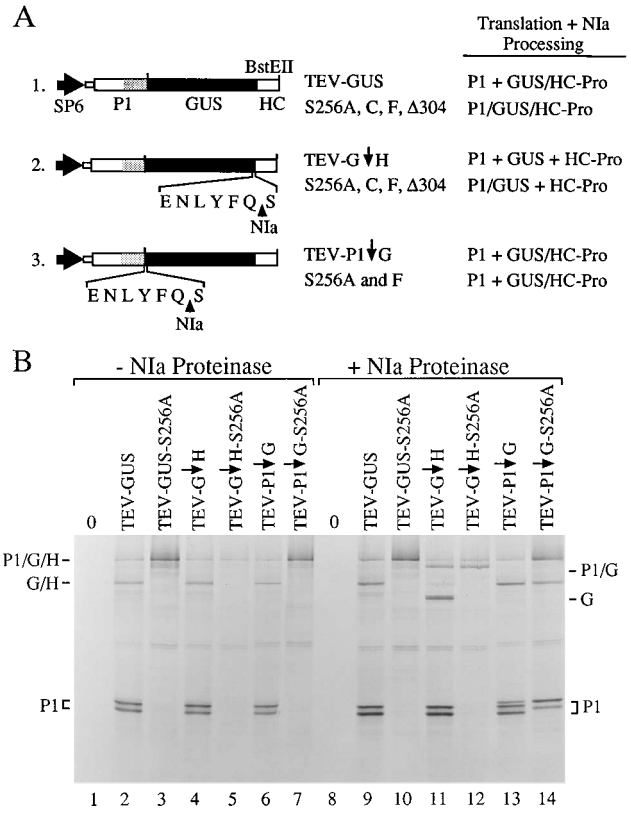

FIG. 6. Insertion of sequences encoding NIa proteinase cleavage sites into parental and P1 mutant genomes. (A) Diagrammatic representation of relevant portions of plasmids containing the introduced cleavage site sequences. Three sets of plasmids were produced. In set 1, parental TEV-GUS and its S256A, C, F and Δ304 mutant derivatives were the same as those shown in Fig. 1 and 2. In set 2, TEV-G ↓ H and its mutant derivatives encoded the NIa cleavage recognition sequence E-N-L-Y-F-Q-S between the GUS and HC-Pro coding regions indicated below the plasmid diagrams. In set 3, TEV-P1 ↓ G and its S256A and F derivatives encoded the NIa cleavage recognition sequence between the P1 and GUS coding regions. The exact position of NIa cleavage between the Q and S residues is indicated. Expected translation and processing products derived from each plasmid are indicated on the right. (B) Cell-free translation and processing products encoded by *Bst*EII-linearized transcripts from TEV-GUS, TEV-G ↓ H, and TEV-P1 ↓ G and the corresponding S256A mutant derivatives of each. [^{35}S]methionine-labeled proteins were synthesized in a wheat germ extract for 1 h. Half of each reaction mix was treated for an additional 1 h with either water (lanes 1 to 7) or NIa proteinase (lanes 8 to 14), and radiolabeled proteins were analyzed by SDS–12.5% polyacrylamide gel electrophoresis and fluorography. Translation reaction mixes programmed with no RNA are shown in lanes 1 and 8. The electrophoretic positions of the P1/GUS/partial HC-Pro polyprotein (P/G/H), GUS/partial HC-Pro (G/H) fusion protein, and P1 protein, which were produced in reactions in the absence of NIa proteinase, are indicated on the left. The electrophoretic positions of the P1/GUS (P/G), GUS (G), and P1 generated after addition of NIa proteinase are indicated on the right.

TABLE 3. Restoration of infectivity of P1 proteinase-debilitated mutants by insertion of NIa cleavage sites

Inoculum	No. of plants infected/no. inoculated[a]		No. of products sequenced[b]	Total no. of plants infected/total no. inoculated[c]
	Immunoblot	RT-PCR		
TEV-GUS	19/19	5/5	2	24/24
TEV-G ↓ H	9/9	3/3	1	12/12
TEV-P1 ↓ G	17/21	7/7	2	24/28
TEV-GUS/S256A	0/5	0/8		0/13
TEV-G ↓ H/S256A	6/6	7/7	3	13/13
TEV-P1 ↓ G/S256A	4/8	7/7	3	11/15
TEV-GUS/Δ304	0/14	0/2		0/16
TEV-G ↓ H/Δ304	5/17	4/5	2	9/22
TEV-GUS/C	0/10	1/4	1	1/10
TEV-G ↓ H/C	9/10	4/4	2	9/10
TEV-GUS/F	0/11	0/7		0/18
TEV-G ↓ H/F	0/9	0/9		0/18
TEV-P1 ↓ G/F	3/12	2/6	2	5/18

[a] Immunoblot analysis was conducted with antibodies against GUS, HC-Pro, and capsid protein. RT-PCR was carried out with RNA isolated from crude virion preparations.

[b] The sequences through the sites of mutation and cleavage site insertion in the P1 mutant genomes and at the corresponding positions in the parental TEV-GUS genome were confirmed by using the RT-PCR products generated from RNA templates isolated from crude virion preparations. The numbers of RT-PCR products sequenced from independent plants are given. The P1 mutations and NIa cleavage sites were confirmed in all RT-PCR products sequenced.

[c] With the exception of the C mutant series, different plants were subjected to immunoblot and RT-PCR analyses. For the C mutants, all plants were analyzed by immunoblot, and a subset were also analyzed by RT-PCR.

G ↓ H/Δ304 mutant infected 41% of inoculated plants (Table 3). Immunoblot analysis with anti-GUS and anti-HC-Pro sera indicated that the NIa cleavage sites were processed properly in each set of infected plants (data not shown). Although the TEV-GUS/F mutant was noninfectious, viability was restored by insertion of the NIa cleavage site between P1 and GUS in TEV-P1 ↓ G/F, as revealed by 25% infected plants. Interestingly, no plants were infected after inoculation with TEV-G ↓ H/F transcripts encoding the NIa cleavage site between GUS and HC-Pro (Table 3). The nonviability of TEV-G ↓ H/F was shown to be a result solely of the F mutation rather than a cryptic mutation elsewhere in the genome, as a site-specific revertant with the wild-type sequence restored was fully infectious (data not shown). Sequence analysis of RT-PCR products from each of the infectious modified genomes indicated that the S256A, Δ304, and F mutations were retained in the progeny, as were the introduced NIa cleavage site sequences. These results indicate that neither P1 proteolytic activity nor a functional P1 proteinase cleavage site is necessary for virus infectivity, provided that separation of P1 from HC-Pro is catalyzed by another proteinase.

Systemic infection was detected in 1 of 10 plants inoculated with TEV-GUS/C at 14 d.p.i. The RT-PCR analysis of the infected plant yielded a relatively weak signal, and the immunoblot assay failed to detect capsid protein (Table 3), indicating that virus accumulation was extremely low. In contrast, 90% of plants inoculated with the TEV-G ↓ H/C transcripts were infected systemically, as revealed by strong immunoblot and RT-PCR signals (Table 3). These data suggest that infectivity was enhanced by insertion of the NIa cleavage site. Surprisingly, immunoblot analysis with anti-GUS serum revealed that free GUS accumulated in TEV-G ↓ H/C-infected plants (Fig. 7, lane 4), just as in plants infected by parental TEV-G ↓ H encoding a wild-type P1 proteinase (lanes 2 and 3). This indicates that the P1 proteinase containing the C insertion was active in vivo, in contrast to its activity in vitro (Fig. 1). However, the relative efficiency of the C mutant proteinase relative to the wild-type proteinase could not be determined.

DISCUSSION

A variety of mutations were introduced into the P1 coding sequence of TEV. Mutants that encoded an active P1 proteinase had no identifiable phenotype distinct from that of parental virus in protoplasts and plants. The most dramatic mutations

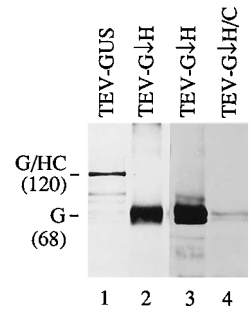

FIG. 7. Immunoblot analysis of parental and mutant TEV-GUS-infected plants. Total SDS-soluble proteins were extracted from systemic leaves of plants infected by the viruses indicated above each lane. The immunoblots were probed with anti-GUS serum. The electrophoretic positions of GUS-containing proteins and their molecular masses (in kilodaltons) are indicated on the left. Note that TEV-GUS encodes a stable GUS/HC-Pro (G/HC) fusion protein (lane 1), whereas TEV-G ↓ H encodes a GUS/HC-Pro polyprotein that undergoes NIa-mediated proteolysis to yield mature-size GUS (G, lanes 2 and 3). Only mature-size GUS was detected in TEV-G ↓ H/C-infected plants (lane 4).

that had little effect were the Δ05 and Δ06 deletions, which removed most of the hypervariable N-terminal half of P1. Not surprisingly, insertions of tripeptides into the nonproteolytic domain also had no effects. These data clearly indicate that the N-terminal half of P1, as well as the RNA sequence coding for this region, are nonessential for TEV replication or movement in plants. While the role of this P1 domain is unclear, it may provide a regulatory function involved in fine tuning of the viral replicative cycle. This domain may also exert a quantitative effect on putative functions of the C-terminal domain (see below) by influencing P1 properties such as turnover or structural stability.

Conversely, mutants that encoded a defective P1 proteinase were debilitated in plants. Infectivity was abolished by the S256A, F, and Δ304 mutations, whereas the C mutation limited the extent of systemic infection and increased the time required for spread compared with the parental virus. These data are most easily interpreted to indicate that either P1 proteolytic activity or excision of P1 from the remainder of the viral polyprotein is necessary for infectivity.

The infectivity of the P1 proteinase-debilitated S256A, F, and Δ304 mutants was restored by second-site mutations resulting in insertion of a cleavage site recognized by the TEV NIa proteinase. In this sense, it is appropriate to consider the NIa cleavage site insertions as gain-of-function suppressor mutations. The S256A mutation was suppressed by cleavage site insertions either between P1 and GUS or between GUS and HC-Pro. Several conclusions can be drawn from these results. First, the P1 proteinase activity is not intrinsically required, as a heterologous proteinase activity can substitute for the normal P1 processing function. Second, TEV infectivity does not depend on the P1 proteinase to catalyze proteolysis at other sites. If P1 processing was required at additional positions, insertion of the NIa cleavage sites only between P1 and HC-Pro would not have rescued all P1 processing defects. Third, separation of P1 from HC-Pro appears to be essential. In fact, from the S256A restoration results, it appears that the exact site of processing to separate P1 from HC-Pro is not critical.

If the proteinase activity of P1 is not intrinsically required, why must P1 be separated from HC-Pro? We suggest that the functions of HC-Pro and/or putative nonproteolytic functions of P1 are debilitated when both P1 and HC-Pro are fused within the same polyprotein. Failure to process may result in mislocalization of one or both proteins within the cell. Alternatively, a processing defect may result in inactivation of HC-Pro biochemical activities. HC-Pro carries out a number of functions during the infection process. The C-terminal one-third constitutes a cysteine-type proteolytic domain required for autoproteolysis between HC-Pro and P3 (5). However, previous results indicated that fusion of P1 to HC-Pro has no effect on HC-Pro proteolytic function (38). The N-terminal region of HC-Pro contains determinants necessary for aphid transmissibility of the virus, although this function is not required for virus viability (3, 35). On the other hand, a number of potyvirus mutants with substitutions or deletions within the N-terminal two-thirds of HC-Pro exhibit replication defects in protoplasts and plants (3, 14), suggesting that HC-Pro also performs a role in genome amplification or gene expression.

In addition to debilitating HC-Pro, inhibition of processing between P1 and HC-Pro may also inactivate a putative nonproteolytic function of P1. It is logical to propose that the P1 protein carries out functions in addition to merely separating itself from HC-Pro. Purified P1 protein expressed in *E. coli* exhibits single-stranded-RNA-binding activity (4), although the role of this activity during potyvirus genome expression or amplification is not clear. In addition, the genetic data presented here support the hypothesis that the P1 proteolytic domain is multifunctional. The S256A mutation was suppressed relatively efficiently by NIa cleavage site insertions at multiple positions, while the F mutation was suppressed inefficiently, and only by insertion of the cleavage site between P1 and GUS. The differential effects of the S256A and F mutations may be interpreted to mean that the P1 C-terminal domain is involved in proteolytic and nonproteolytic functions. Such results would be predicted if the S256A mutation inhibited only P1 proteolytic activity and the F mutation altered proteolytic and nonproteolytic functions.

Does the P1 protein play a direct role in intercellular movement of TEV? Despite considerable speculation (16, 24, 32, 33), experimental evidence implicating the P1 protein as a transport factor is lacking. To date, only the capsid protein has been shown to be required for virus movement in plants (13). While the slow-infection phenotype of the C mutant might indicate that P1 functions directly in movement, an alternative scenario seems more likely. The slow-infection phenotype was suppressed by NIa cleavage site insertion, indicating that the C mutant defect was a function of protein processing rather than debilitation of a "movement domain" within P1. Immunoblot analysis of plants infected by a virus containing the C mutation, however, revealed that the P1 proteinase was, in fact, functional in vivo. These findings can be reconciled by proposing that the P1 proteinase encoded by the C mutant was not inhibited completely, but rather possessed a slow processing activity that indirectly affected other P1 and/or HC-Pro functions required for infectivity. Given the variety of P1 mutants that failed to exhibit specific defects in intercellular movement, it seems doubtful that P1 plays an integral role in virus transport.

ACKNOWLEDGMENTS

We thank Ruth Haldeman-Cahill and Patricia Valdez for assistance with maintenance of plants; Bruce McDonald for help with the statistics; and Mary Schaad, Xiao Hua Li, Kristin Kasschau, and Sunita Mahajan for helpful comments on the manuscript.

This research was supported by the National Research Initiative Competitive Grants Program of the U.S. Department of Agriculture (91-37303-6435), the National Science Foundation (IBN-9158559), and the National Institutes of Health (AI27832).

REFERENCES

1. **Allison, R., R. E. Johnston, and W. G. Dougherty.** 1986. The nucleotide sequence of the coding region of tobacco etch virus genomic RNA: evidence for the synthesis of a single polyprotein. Virology **154:**9–20.
2. **Andino, R., G. E. Rieckhof, P. L. Achacoso, and D. Baltimore.** 1993. Poliovirus RNA synthesis utilizes an RNP complex formed around the 5′-end of viral RNA. EMBO J. **12:**3587–3598.
3. **Atreya, C. D., P. L. Atreya, D. W. Thornbury, and T. P. Pirone.** 1992. Site-directed mutations in the potyvirus HC-PRO gene affect helper component activity, virus accumulation, and symptom expression in infected tobacco plants. Virology **191:**106–111.
4. **Brantley, J. D., and A. G. Hunt.** 1993. The N-terminal protein of the polyprotein encoded by the potyvirus tobacco vein mottling virus is an RNA binding protein. J. Gen. Virol. **74:**1157–1162.
5. **Carrington, J. C., S. M. Cary, T. D. Parks, and W. G. Dougherty.** 1989. A second proteinase encoded by a plant potyvirus genome. EMBO J. **8:**365–370.
6. **Carrington, J. C., and W. G. Dougherty.** 1987. Small nuclear inclusion protein encoded by a plant potyvirus genome is a protease. J. Virol. **61:**2540–2548.
7. **Carrington, J. C., and W. G. Dougherty.** 1988. A viral cleavage site cassette: identification of amino acid sequences required for tobacco etch virus polyprotein processing. Proc. Natl. Acad. Sci. USA **85:**3391–3395.
8. **Carrington, J. C., and D. D. Freed.** 1990. Cap-independent enhancement of translation by a plant potyvirus 5′ nontranslated region. J. Virol. **64:**1590–1597.
9. **Carrington, J. C., D. D. Freed, and C.-S. Oh.** 1990. Expression of potyviral polyproteins in transgenic plants reveals three proteolytic activities required for complete processing. EMBO J. **9:**1347–1353.
10. **Carrington, J. C., R. Haldeman, V. V. Dolja, and M. A. Restrepo-Hartwig.** 1993. Internal cleavage and *trans*-proteolytic activities of the VPg-proteinase (NIa) of tobacco etch potyvirus in vivo. J. Virol. **67:**6995–7000.
11. **Choi, H.-K., L. Tong, W. Minor, P. Dumas, U. Boege, M. G. Rossmann, and G. Wengler.** 1991. Structure of Sindbis virus core protein reveals a chymotrypsin-like serine proteinase and the organization of the virion. Nature (London) **354:**37–43.
12. **Dolja, V. V., and J. C. Carrington.** 1992. Evolution of positive-strand RNA viruses. Semin. Virol. **3:**315–326.
13. **Dolja, V. V., R. Haldeman, N. L. Robertson, W. G. Dougherty, and J. C. Carrington.** 1994. Distinct functions of capsid protein in assembly and movement of tobacco etch potyvirus in plants. EMBO J. **13:**1482–1491.
14. **Dolja, V. V., K. L. Herndon, T. P. Pirone, and J. C. Carrington.** 1993. Spontaneous mutagenesis of a plant potyvirus genome after insertion of a foreign gene. J. Virol. **67:**5968–5975.
15. **Dolja, V. V., H. J. McBride, and J. C. Carrington.** 1992. Tagging of plant potyvirus replication and movement by insertion of β-glucuronidase into the viral polyprotein. Proc. Natl. Acad. Sci. USA **89:**10208–10212.
16. **Domier, L. L., J. G. Shaw, and R. E. Rhoads.** 1987. Potyviral proteins share amino acid sequence homology with picorna-, como-, and caulimoviral proteins. Virology **158:**20–27.
17. **Dougherty, W. G., J. C. Carrington, S. M. Cary, and T. D. Parks.** 1988. Biochemical and mutational analysis of a plant virus polyprotein cleavage site. EMBO J. **7:**1281–1287.
18. **Dougherty, W. G., and E. Hiebert.** 1980. Translation of potyvirus RNA in a rabbit reticulocyte lysate: reaction conditions and identification of capsid protein as one of the products of *in vitro* translation of tobacco etch and pepper mottle viral RNAs. Virology **101:**466–474.
19. **Dougherty, W. G., and T. D. Parks.** 1989. Molecular genetic and biochemical evidence for the involvement of the heptapeptide cleavage sequence in determining the reaction profile at two tobacco etch virus cleavage sites in cell-free assays. Virology **172:**145–155.
20. **Dougherty, W. G., and T. D. Parks.** 1991. Post-translational processing of the tobacco etch virus 49-kDa small nuclear inclusion polyprotein: identification of an internal cleavage site and delimitation of VPg and proteinase domains. Virology **183:**449–456.
21. **Dougherty, W. G., and B. L. Semler.** 1993. Expression of virus-encoded proteinases: functional and structural similarities with cellular enzymes. Microbiol. Rev. **57:**781–822.
22. **Jefferson, R. A., T. A. Kavanagh, and M. W. Bevan.** 1987. GUS fusions: β-glucuronidase as a sensitive and versatile gene fusion marker in higher plants. EMBO J. **6:**3901–3907.
23. **Kunkel, T. A., J. D. Roberts, and R. Zakour.** 1987. Rapid and efficient site-specific mutagenesis without phenotypic selection. Methods Enzymol. **154:**367–382.
24. **Laín, S., J. L. Riechmann, and J. A. García.** 1989. The complete nucleotide sequence of plum pox potyvirus RNA. Virus Res. **13:**157–172.
25. **Mavankal, G., and R. E. Rhoads.** 1991. In vitro cleavage at or near the N-terminus of the helper component protein in the tobacco vein mottling virus polyprotein. Virology **185:**721–731.
26. **Murphy, J. F., R. E. Rhoads, A. G. Hunt, and J. G. Shaw.** 1990. The VPg of tobacco etch virus RNA is the 49 kDa proteinase or the N-terminal 24 kDa part of the proteinase. Virology **178:**285–288.
27. **Negrutiu, I., R. Shillito, I. Potrykus, G. Biasini, and F. Sala.** 1987. Hybrid genes in the analysis of transformation conditions. 1. Setting up a simple method for direct gene transfer in plant protoplasts. Plant Mol. Biol. **8:**363–373.
28. **Oh, C.-S., and J. C. Carrington.** 1989. Identification of essential residues in potyvirus proteinase HC-Pro by site-directed mutagenesis. Virology **173:**692–699.
29. **Parks, T. D., K. K. Leuther, E. D. Howard, S. A. Johnston, and W. G. Dougherty.** 1994. Release of proteins and peptides from fusion proteins using a recombinant plant virus proteinase. Anal. Biochem. **216:**413–417.
30. **Restrepo, M. A., D. D. Freed, and J. C. Carrington.** 1990. Nuclear transport of plant potyviral proteins. Plant Cell **2:**987–998.
31. **Restrepo-Hartwig, M. A., and J. C. Carrington.** 1994. The tobacco etch potyvirus 6-kilodalton protein is membrane associated and involved in viral replication. J. Virol. **68:**2388–2397.
32. **Riechmann, J. L., S. Laín, and J. A. García.** 1992. Highlights and prospects of potyvirus molecular biology. J. Gen. Virol. **73:**1–16.
33. **Robaglia, C., M. Durand-Tardif, M. Tronchet, G. Boudazin, S. Astier-Manifacier, and F. Casse-Delbart.** 1989. Nucleotide sequence of potato virus Y (N strain) genomic RNA. J. Gen. Virol. **70:**935–947.
34. **Shahabuddin, M., J. G. Shaw, and R. E. Rhoads.** 1988. Mapping of the tobacco vein mottling virus VPg cistron. Virology **163:**635–637.
35. **Thornbury, D. W., C. A. Patterson, J. T. Dessens, and T. P. Pirone.** 1990. Comparative sequences of the helper component (HC) region of potato virus Y and a HC-defective strain, potato virus C. Virology **178:**573–578.
36. **Vance, V. B., D. Moore, T. H. Turpen, A. Bracker, and V. C. Hollowell.** 1992. The complete nucleotide sequence of pepper mottle virus genomic RNA: comparison of the encoded polyprotein with those of other sequences potyviruses. Virology **191:**19–30.
37. **Verchot, J., K. L. Herndon, and J. C. Carrington.** 1992. Mutational analysis of the tobacco etch potyviral 35-kDa proteinase: identification of essential residues and requirements for autoproteolysis. Virology **190:**298–306.
38. **Verchot, J., E. V. Koonin, and J. C. Carrington.** 1991. The 35-kDa protein from the N-terminus of a potyviral polyprotein functions as a third virus-encoded proteinase. Virology **185:**527–535.

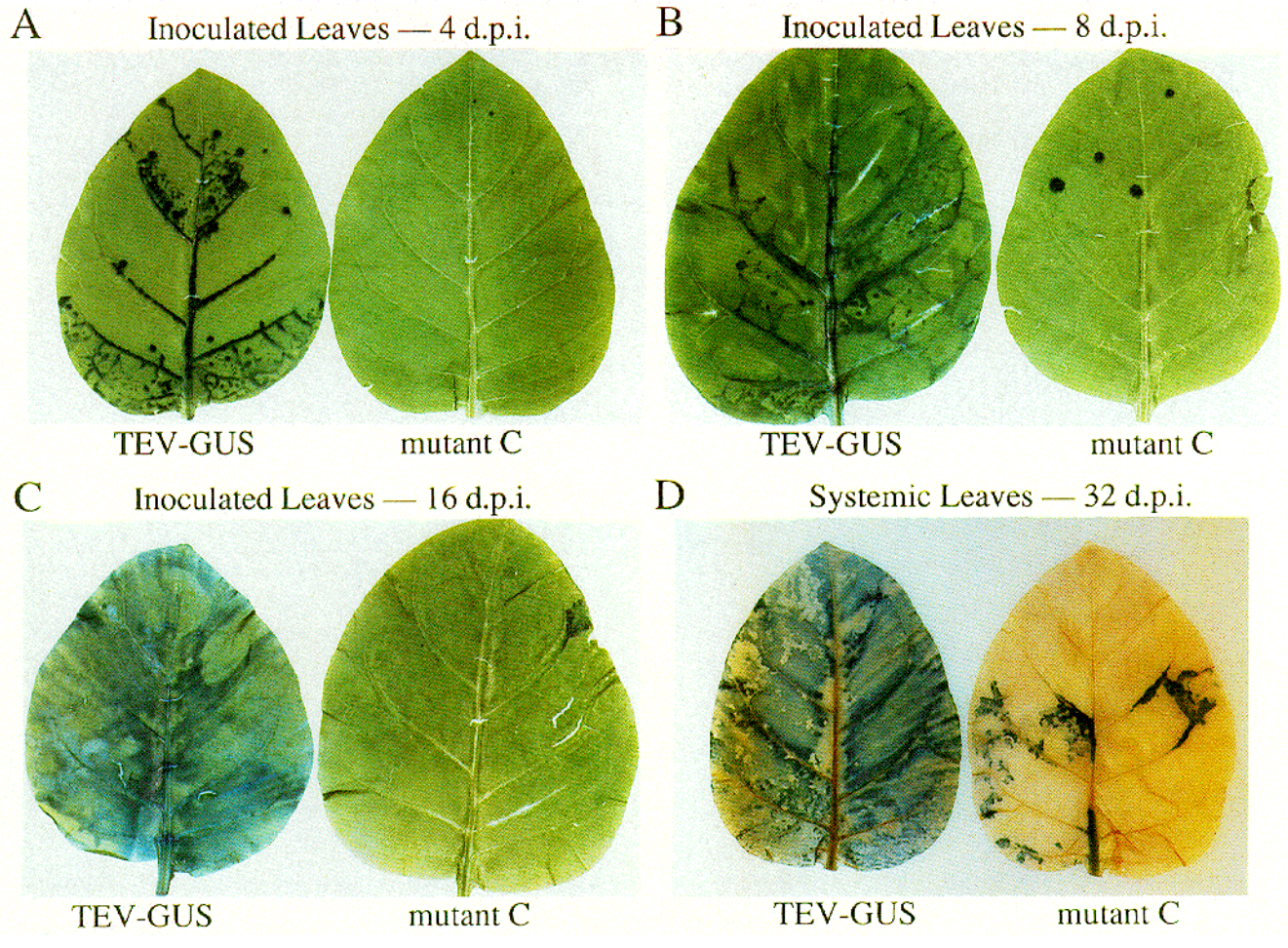
A
Inoculated Leaves — 4 d.p.i.
TEV-GUS
mutant C
B
Inoculated Leaves — 8 d.p.i.
TEV-GUS
mutant C
C
Inoculated Leaves — 16 d.p.i.
TEV-GUS
mutant C
D
Systemic Leaves — 32 d.p.i.
TEV-GUS
mutant C